

## Charge reduction stabilizes intact membrane protein complexes for mass spectrometry

Shahid Mehmood, Julien Marcoux, Jonathan T.S. Hopper, Timothy M. Allison, Idir Liko, Antoni J. Borysik, and Carol V. Robinson\*

### Materials and Methods

*AmtB Expression and Purification:* AmtB was expressed and purified as described previously.<sup>1</sup> Briefly, MBP–AmtB plasmid was transformed into *E. coli* BL21 (DE3) Gold (Agilent). After cell lysis and centrifugation, cell membranes were solubilised in OG detergent. Detergent solubilised MBP–AmtB was purified using a 5 ml HisTrap-HP column followed by overnight cleavage of His-tag by TEV protease. The uncut fusion protein and TEV were removed by reverse affinity using 5 ml HisTrap column. After concentrating, the AmtB protein was either used immediately or flash-frozen in liquid nitrogen and stored at  $-80^{\circ}\text{C}$ .

*Ion mobility mass spectrometry:* Membrane proteins were buffer exchanged to 200 mM ammonium acetate supplemented with 1% OG for OmpF and AmtB and 0.02 % DDM for P-gp. The samples were introduced into a modified Synapt2,<sup>2</sup> according to previously reported protocols,<sup>3,4</sup> under the following parameters: capillary 1.5-1.8 kV, cone 100-200 V and trap collision energy 150-200 V. The backing pressure was increased to 5-6 mbar to promote the transmission of high m/z species. The voltage and pressure in the drift cell were set at 50 V and 1.7-1.8 Torr with 40 ml/min of helium, respectively. The temperature outside of the drift cell was monitored with a thermocouple (Omega Engineering).

Mason-Schamp equation,<sup>5</sup>

$$\Omega = \frac{(18\pi)^{\frac{1}{2}}}{16} \frac{ze}{(k_b T)^{\frac{1}{2}}} \frac{1}{N} \frac{t_d V p_0 T}{L^2 p T_0} \sqrt{\frac{1}{\mu}}$$

was used to determine the averaged ion-neutral collision cross section (CCS) ( $\Omega$ ) from ion drift time (td). Theoretical CCSs were calculated using MOBCAL (projection approximation method) and incorporating scaling factor of 1.14, as previously reported.<sup>6</sup>

*Loop modelling and molecular dynamics:* The missing loops of P-gp (PDB: 3G5U),<sup>7</sup> were built using Modeller (8254673) implemented within UCSF Chimera 1.8 (15264254) using the default settings. Of the generated structures the model with the lowest DOPE score was selected for further manipulation by MD. All MD simulations were performed without solvent using the OPLS/AA forcefield implemented within GROMACS 4.5.5 (16211538). First, a steepest descent energy minimization was performed to eliminate unfavorable contacts and steric overlaps. This was directly followed by unrestrained vacuum simulations. Neither periodicity nor cutoffs were used during the calculations. A small integration time step of 1 fs was used to ensure energy conservation, and bonds to H-atoms were constrained using the LINCS algorithm. We used a dielectric constant of  $2\epsilon^{\circ}$  (where  $\epsilon^{\circ}$  is the dielectric permittivity of vacuum). MD simulations were based on a previously published protocol and were performed at 300 K for 2 ns following an 8 ns heating phase to 800 K (22280183). Since the purpose of the MD was to provide a yardstick for collapsed conformations all simulations were carried out on charge neutral species. Guided loop collapse of 3GU5 was performed at 300 K with heavy position restraints on all atoms except those involved in modelled loop regions.

*P-gp cardiolipin binding experiments:* Four different concentrations of cardiolipin CL14 were incubated with DDM detergent solubilized fixed concentration of P-gp for five minutes. This was followed immediately by analysis on a Q-ToF2 mass spectrometer under identical activation conditions. Solutions of cardiolipin were prepared according to a previously described protocol.<sup>1</sup> A control experiment was also included in which a carbohydrate, oligomannose 9 (Man-9), known not to bind to P-gp was incubated in solution and mass spectra recorded under 'normal' ES and charge reduced conditions. No binding was observed in either case.

*Circular dichroism:* Circular dichroism spectra of P-gp were assessed at a protein concentration of 0.5 mg/mL in ammonium acetate buffer with and without 10 mM imidazole at 20 °C. The scans were performed from 260 to 200 nm at a bandwidth of 1 nm with a scanning speed of 50 nm/min. Data were smoothed using the Savitzky-Golay algorithm of the Jasco Spectrum Manager.

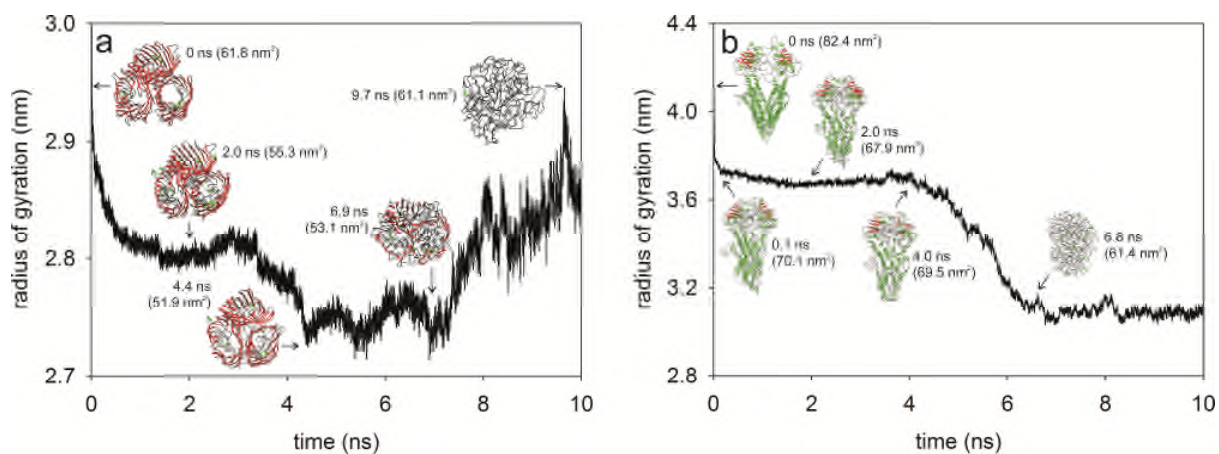


**Figure S1.** MD trajectories and selected structures of OmpF (a) and P-gp (b). MD simulations were performed on charge neutral species at 300 K (0 – 2 ns) followed by a linear increase to 800 K (2 – 10 ns) as described (Methods). Collision cross section ( $\Omega$ ) of selected structures were obtained using projection approximation method implemented in MOBCAL after correcting with scaling factor.<sup>8</sup>

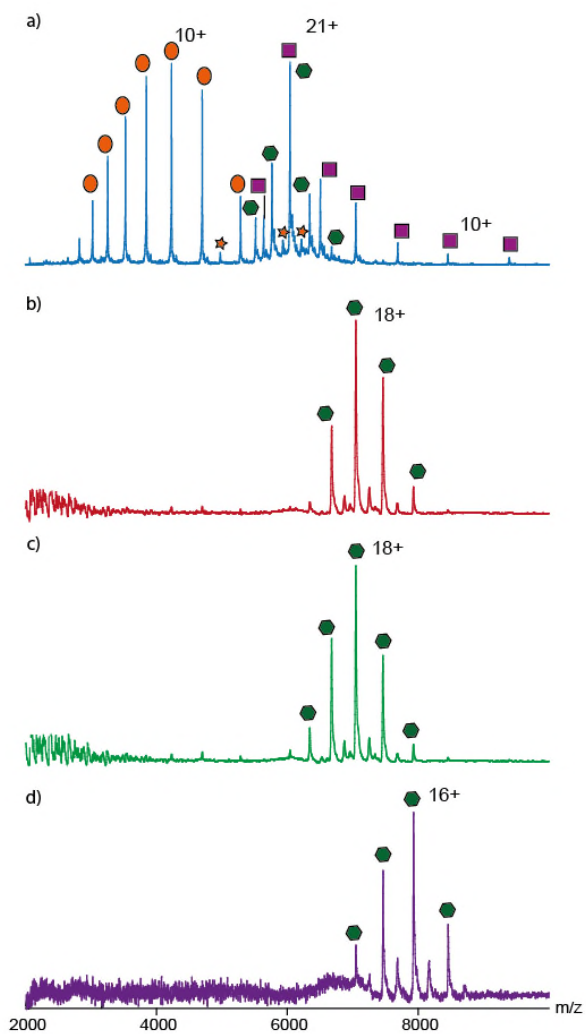


**Figure S2.** Mass spectra of AmtB under normal conditions (a), ACN exposed (b), Imidazole added in protein solution (c) and both ACN exposed and imidazole added in solution (d). Charge state peaks are labeled as follows: Unassigned peaks (orange star), monomer (orange circle), dimer (violet square) and trimer (green diamond). A decrease in signal intensity was observed upon charge reduction, attributed to a reduction in ion transmission of the charge-reduced trimer. Deconvolution of the charge states under normal conditions exhibited 67 %, 19 % and 14 % population of monomer, dimer and trimer respectively.

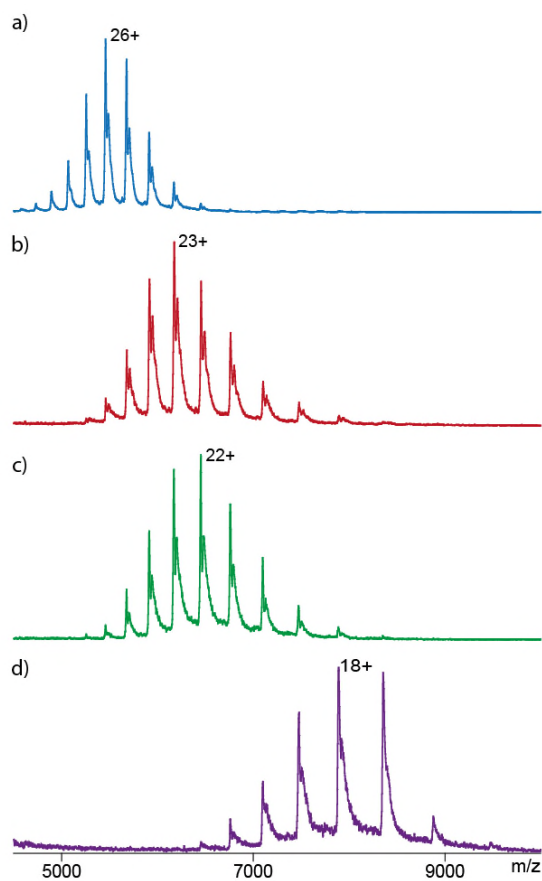


**Figure S3.** Mass spectra of P-gp under normal conditions (a), ACN exposed (b), Imidazole added in protein solution (c) and both ACN exposed and imidazole added in protein solution (d).

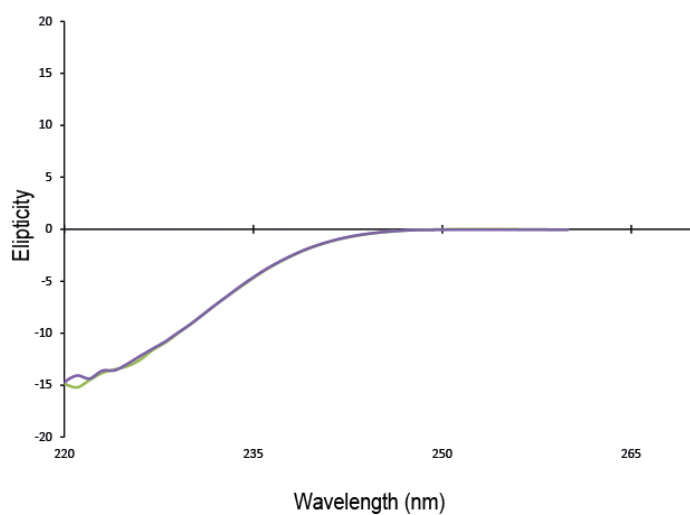


**Figure S4.** CD spectroscopy of P-gp prior (green line) and after (violet line) addition of imidazole in protein solution. The addition of imidazole did not affect overall topology of the protein as evident by secondary structure conservation.

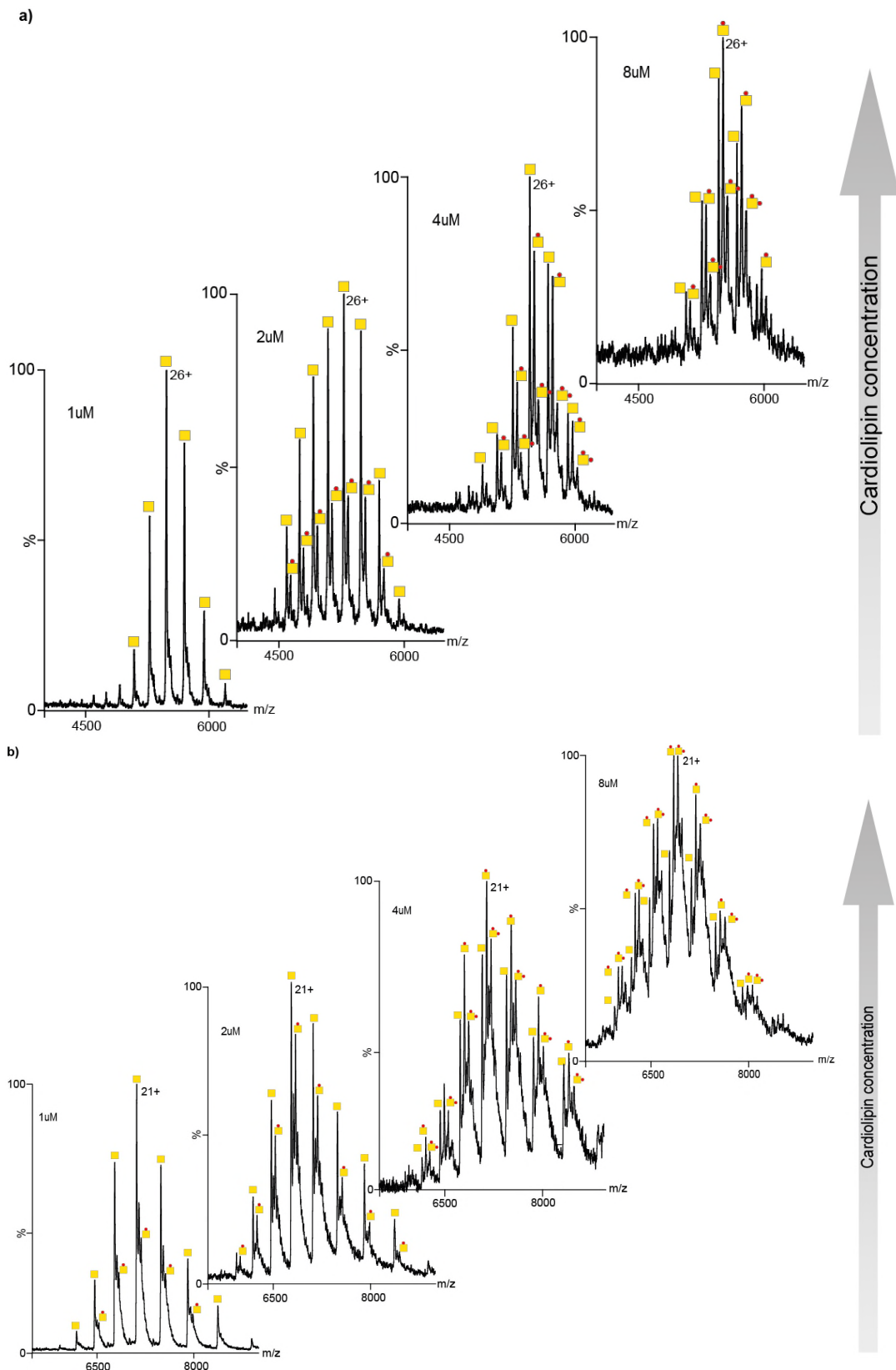
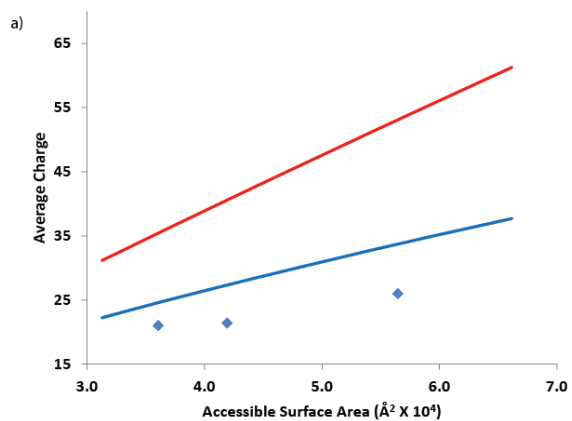
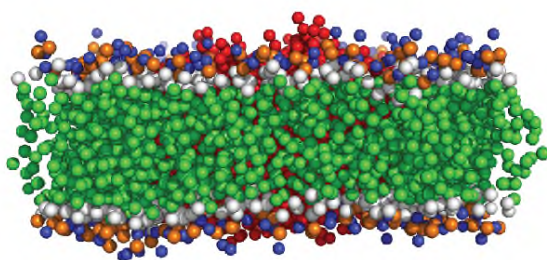


**Figure S5.** Cardiolipin CL14 binding to P-gp. Mass spectra showing binding of cardiolipin to a fixed concentration of P-gp; under normal conditions (ammonium acetate buffer) (a) and charge reduced conditions (b). For the charge reduced species the lipid bound state is more prevalent than the apo form. By contrast at the higher charge states apo protein predominates. Increased binding of CL is evident for the lower charge state species with more native-like structures. Charge state peaks are labeled as follows: Apo protein (yellow square), one CL14 bound (yellow square with one small red circle) and two CL14 bound species (yellow square with two small red circles).



b) AmtB: MW= 126 kDa, Average CS= 21+



c) ABC transporter: MW= 141 kDa, Average CS= 26+

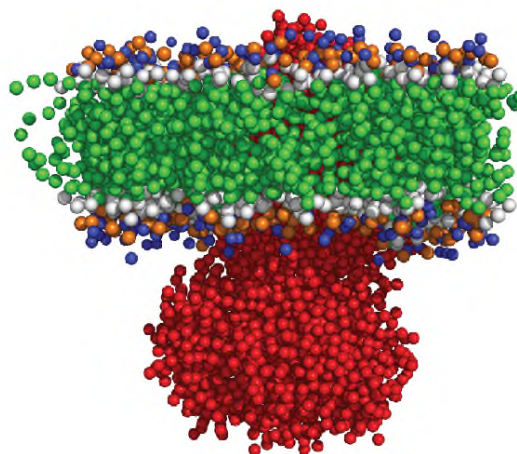


**Figure S6.** The relationship between charge state and accessible surface area of native-like (blue lines) and denatured (red lines) soluble proteins.<sup>9</sup> Light blue diamonds are the membrane proteins analyzed in this study (a). Predicted lipid bilayer around AmtB (b) and ABC transporter Sav 1866 (c) a bacterial homolog of P-gp.<sup>9</sup>

**Table S1**

	<b>OmpF</b>	<b>AmtB</b>	<b>P-gp</b>
Molecular weight calculated	111252 Da	126833 Da	141699 Da
Molecular weight experimental	111300 ± 5 Da	126825 ± 15 Da	141893 ± 17 Da
"Standard conditions" average z	22 ± 0.2	21 ± 0.4	26 ± 0.3
ACN expose-Imidazole added average z	16.1 ± 0.2	16.5 ± 0.8	18.1 ± 0.3
CCS calculated (native-like)	6180 Å <sup>2</sup>	5833 Å <sup>2</sup>	8240 Å <sup>2</sup>
CCS experimental (native-like)	6300 ± 102 Å <sup>2</sup>	7200 ± 210 Å <sup>2</sup>	8200 ± 40 Å <sup>2</sup>
CCS calculated (collapsed)	5190 Å <sup>2</sup>	-	7010 Å <sup>2</sup>
CCS experimental (collapsed)	5155 ± 28 Å <sup>2</sup>	-	7420 ± 57 Å <sup>2</sup>
Detergent	OG	OG	DDM

**References:**

- (1) Laganowsky, A.; Reading, E.; Allison, T. M.; Ulmschneider, M. B.; Degiacomi, M. T.; Baldwin, A. J.; Robinson, C. V. *Nature* **2014**, *510*, 172.
- (2) Bush, M. F.; Hall, Z.; Giles, K.; Hoyes, J.; Robinson, C. V.; Ruotolo, B. T. *Anal. Chem.* **2010**, *82*, 9557.
- (3) Hernandez, H.; Robinson, C. V. *Nat. Protoc.* **2007**, *2*, 715.
- (4) Ruotolo, B. T.; Benesch, J. L.; Sandercock, A. M.; Hyung, S. J.; Robinson, C. V. *Nat. Protoc.* **2008**, *3*, 1139.
- (5) Mason, E. A.; Schamp Jr, H. W. *Annals of Physics* **1958**, *4*, 233.
- (6) Hall, Z.; Politis, A.; Robinson, Carol V. *Structure* **2012**, *20*, 1596.
- (7) Aller, S. G.; Yu, J.; Ward, A.; Weng, Y.; Chittaboina, S.; Zhuo, R.; Harrell, P. M.; Trinh, Y. T.; Zhang, Q.; Urbatsch, I. L.; Chang, G. *Science* **2009**, *323*, 1718.
- (8) Hall, Z.; Politis, A.; Bush, M. F.; Smith, L. J.; Robinson, C. V. *J. Am. Chem. Soc.* **2012**, *134*, 3429.
- (9) Testa, L.; Brocca, S.; Grandori, R. *Anal. Chem.* **2011**, *83*, 6459.